

Comparison of Transient Electron Heat Transport in LHD Helical and JT-60U Tokamak Plasmas

S. Inagaki¹, H. Takenaga², K. Ida¹, A. Isayama², N. Tamura¹, T. Takizuka², T. Shimozuma¹, Y. Kamada², S. Kubo¹, Y. Miura², Y. Nagayama¹, K. Kawahata¹, S. Sudo¹, K. Ohkubo¹,
LHD Experimental Group and the JT-60U Team

- 1) National Institute for Fusion Science, Oroshi-cho, Toki-shi, Gifu, 509-5292, Japan
2) Naka Fusion Research Establishment, Japan Atomic Energy Research Institute, Naka-machi, Naka-gun, Ibaraki 311-0193, Japan

e-mail contact of main author : inagaki@LHD.nifs.ac.jp

Abstract. Transient transport experiments are performed in plasmas with and without Internal Transport Barrier (ITB) on LHD and JT-60U. The dependence of χ_e on electron temperature, T_e , and electron temperature gradient, ∇T_e , is analyzed by an empirical non-linear heat transport model. In plasmas without ITB, two different types of non-linearity of the electron heat transport are observed from cold/heat pulse propagation. The χ_e depends on T_e and ∇T_e in JT-60U, while the ∇T_e dependence is weak in LHD. Inside the ITB region, there is no or weak ∇T_e dependence both in LHD and JT-60U. A cold pulse growing driven by the negative T_e dependence of χ_e is observed inside the ITB region (LHD) and near the boundary of the ITB region (JT-60U).

1. Introduction

Helical systems and tokamaks are the most realistic concepts for magnetic confinement of thermonuclear plasmas. There are some similarities and differences in heat transport between helical systems and tokamaks. Similarities in transport are as following: (i) the radial heat transport is anomalously higher than neoclassical theory, (ii) the global energy confinement time shows similar parametric dependence and the power degradation of confinement is observed in both devices. Heat (and particle) transport in both devices are also considered to be driven by turbulent processes. On the other hand, one of the differences in heat transport is as following: the T_e profile reacts weakly to changes of the heating deposition profile in tokamaks, however, this transport phenomenon, known as “profile stiffness” [1, 2], is weak or absent in helical systems. In fact, although the global confinement scaling is similar to ELMy H-mode scaling [3], no evidence for the tokamak-like stiffness is observed in the Large Helical Device (LHD). The physical models that can explain stiffness can be divided into two categories: local and non-local. Some local transport models based on temperature-gradient-driven turbulence indicate that the heat transport is non-linear and thus the electron heat diffusivity, χ_e , has a dependence on T_e and/or ∇T_e [4, 5]. Especially, the non-linear models based on the “critical gradient scale length” can explain some of tokamak-type stiffness [6]. However the “critical gradient scale length” is unclear in the LHD inward shifted configuration (major radius at the magnetic axis, $R_{ax} = 3.5\text{m}$, an averaged plasma radius, $a_p = 0.58\text{m}$). Figure 1 shows the T_e and temperature scale length, $L_T^{-1} = -\nabla T_e/T_e$, dependence of χ_e in the LHD NBI plasmas (neutral beam heating power, $P_{NB} \sim 2\text{-}6\text{MW}$, line averaged density, $\bar{n}_e = 1\text{-}3 \times 10^{19}\text{m}^{-3}$). Although the T_e dependence of χ_e is clear, L_T^{-1} dependence of χ_e is unclear in the power balance analysis. Therefore, the validity of non-linear transport models based on turbulence should be clarified in helical systems. To study the non-linearity of heat transport, transient transport analysis is recognized as a very powerful tool because it can yield $\partial q_e/\partial \nabla T_e$ and $\partial q_e/\partial T_e$ [7]. Thus the transient response should be explained by the first-principle transport models as well as the steady state profiles.

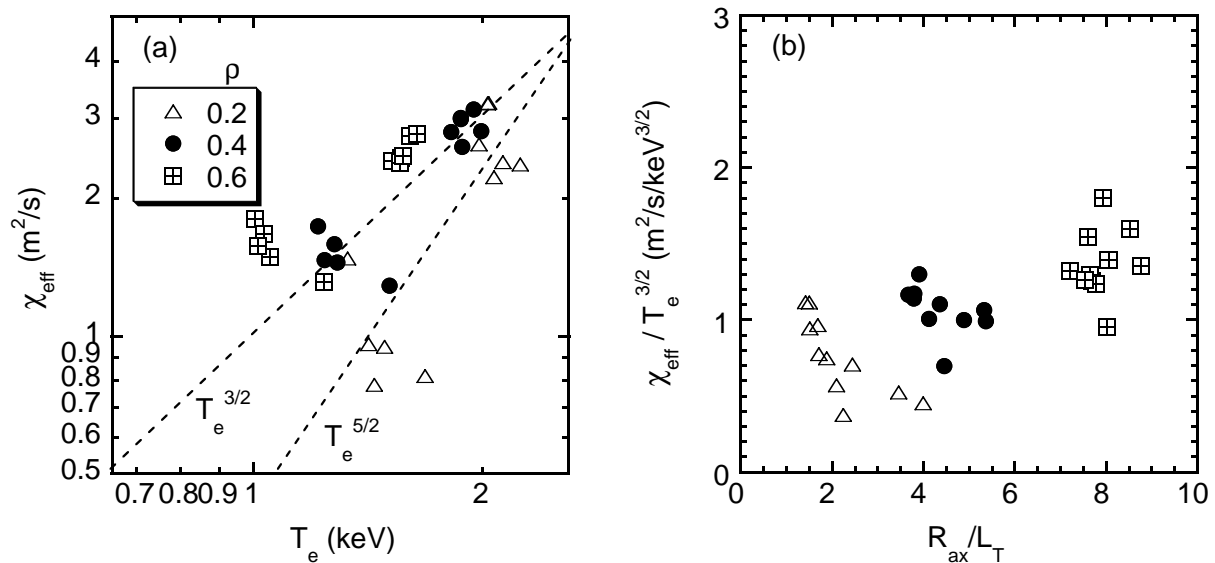


FIG. 1: (a) T_e and (b) L_T dependence of χ_e at different radii in the LHD NBI plasmas. The χ_e is normalized by the gyro-Bohm T_e dependence in (b)

In addition, the transient analysis is the only technique which can obtain information to answer the interesting question of whether transport in magnetically confined plasmas is determined by local plasma parameters or not.

Theoretically, the magnetic configuration influences turbulence in many aspects. Hence, comparison of heat transport features between tokamak and helical systems would reveal the importance of the magnetic configuration for transport and be very useful to gain a comprehensive understanding of the turbulent transport in toroidal devices because their magnetic configurations are quite different (e.g. aspect ratio and safety factor, q , profile). Recent experimental progress on LHD and JT-60U enables us to make more an extensive comparison of the transient response in plasmas not only without ITB but also with ITB. In this paper, the newly obtained results of transient transport experiments are reported and the characteristics of electron transport obtained from transient analysis are compared between LHD and JT-60U plasmas.

2. Transient transport experiments

In order to induce a cold pulse, a tracer encapsulated solid pellet (TESPEL [8]) is injected into the LHD edge. Figure 2(a) shows the typical time evolution of cold pulse induced by TESPEL injection in the low power NBI plasma on LHD (neutral beam injection power $P_{NB} \sim 3$ MW, line averaged density $\bar{n}_e = 2 \times 10^{19} \text{m}^{-3}$). To study the non-linearity between heat flux and temperature gradient in toroidal plasma, the transient transport analysis is carried out with a simple non-linear model for χ_e written as $\chi_e \propto T_e^\alpha |\nabla T_e|^\beta$. By using this model, the perturbed electron heat transport equation can be written as,

$$\frac{3}{2} n_e \frac{\partial \delta T_e}{\partial t} = \nabla \cdot \left(n_e (1 + \beta) \chi_e \nabla \delta T_e - n_e \alpha \chi_e \frac{\delta T_e}{L_T} \right). \quad (1)$$

Here n_e , ∇T_e , T_e and χ_e are static values obtained just before TESPEL injection, $\delta T_e = T_e(r, 0) - T_e(r, t)$ and χ_e can be estimated by the static analysis i.e. power balance analysis. The n_e in-

creases in the ablation region ($\rho > 0.6$) while it doesn't change in core region within the accuracy of the Abel inversion. The particle diffusivity, which is estimated by gas-puff modulation experiments [9], is much smaller than χ_e and thus the particle transport effects on the cold pulse propagation are neglected in LHD. When the heat flux perturbation, $\delta q_e(r, t)$, and the perturbation scale length, $L_{\delta T_e}$, are defined as

$$\delta q_e(r, t) = \frac{1}{r} \int_0^r \frac{3}{2} n_e \frac{\partial \delta T_e}{\partial t} \rho d\rho, \quad L_{\delta T_e}(r, t) = (\nabla \delta T_e / \delta T_e)^{-1},$$

Eq. 1 can be written as

$$\frac{\delta q_e}{n_e \delta T_e} = \frac{\chi_{tr}}{L_{\delta T_e}} - V_{tr}, \quad (2)$$

here $\chi_{tr} = (1 + \beta)\chi_e$, $V_{tr} = \alpha\chi_e L_T^{-1}$ and r is the averaged minor radius. Figure 2(b) shows the time trace of plasma in the gradient - flux space for a cold pulse propagation. The fact that data points indeed lay on a straight line allows us to determine β and α from the slope and intercept of a line. The obtained χ_{tr} is shown in Fig. 2(c). The heat diffusivity estimated by power balance analysis, χ_{pb} , is also shown. The small difference between χ_{pb} and χ_{tr} indicates a weak ∇T_e dependence of χ_e ($\beta \ll 1$) in LHD. On the contrary, the T_e dependence of χ_e is indicated in Fig. 2(d). A gyro-Bohm like T_e dependence ($\alpha = 3/2 - 5/2$) can explain the obtained α . Although the α in the edge region is more important to compare with the global energy confinement and it has not obtained by transient analysis, T_e dependence of χ_e can be considered as one of the candidates to explain the power degradation of the global confinement in LHD [3]. In high NB power cases, however, the non-local T_e rise, which is discussed later, appears and it makes hard to decouple the non-linearity of χ_e from observations.

To perturb the core region of JT-60U plasma, the short pulse (100ms) ECH injection is carried out. Figure 3(a) shows the typical response of T_e to a step of the injected ECH power ($P_{EC} \sim 1\text{MW}$) in the core region. Here, the peak of ECH power deposition is located at $\rho \sim 0.6$, and there is no ECH power source in the region of $\rho < 0.3$. The heat pulse propagates from edge to core similarly to the cold pulse and thus the transient analysis with an empirical non-linear χ_e model, which is discussed above, can be applied (see Fig. 3(b)). The $\chi_{tr} = 0.16\text{m}^2/\text{s}$ is obtained in an ohmic plasma while the χ_{tr} increases in the NBI plasma ($0.24\text{m}^2/\text{s}$) due to the increase in T_e or ∇T_e . To compare the ∇T_e dependence of χ_e with the critical gradient length model, both χ_{tr} and χ_{pb} are plotted as a function of R_{ax}/L_T (see Fig. 3(c)). The χ_{pb} and the χ_{tr} are normalized by $T_e^{3/2}$ to decoupled the gyro-Bohm T_e dependence. The dependence of χ_{pb} on R_{ax}/L_T may be changed at $R_{ax}/L_T = 6 - 8$ i.e. the temperature-gradient-driven mode may be switched on above $R_{ax}/L_T = 6-8$ and χ_e has ∇T_e dependence, and thus the enhancement of χ_{tr} ($\chi_{tr} > \chi_{pb}$) may be observed at $R_{ax}/L_T = 6-8$. The ∇T_e dependence factor β decreases from 3 to 1.6 with the increase in R_{ax}/L_T , while the T_e dependence factor $\alpha = 0.5 - 2$ is not different from that obtained in the LHD plasma.

There are differences in non-linearity of χ_e between LHD and JT-60U plasmas without ITBs. The T_e dependence of χ_e is larger than ∇T_e dependence in LHD plasma. On the other hand, a ∇T_e dependence of χ_e is observed in JT-60U plasma. For the stabilization of micro-turbulence, the local shear is a critical parameter [10]. The influence of local and global shear on turbulence may be one of the candidates to explain the difference in the non-linearity between LHD and JT-60U plasmas.

3. Cold pulse propagations in plasmas with electron internal transport barrier

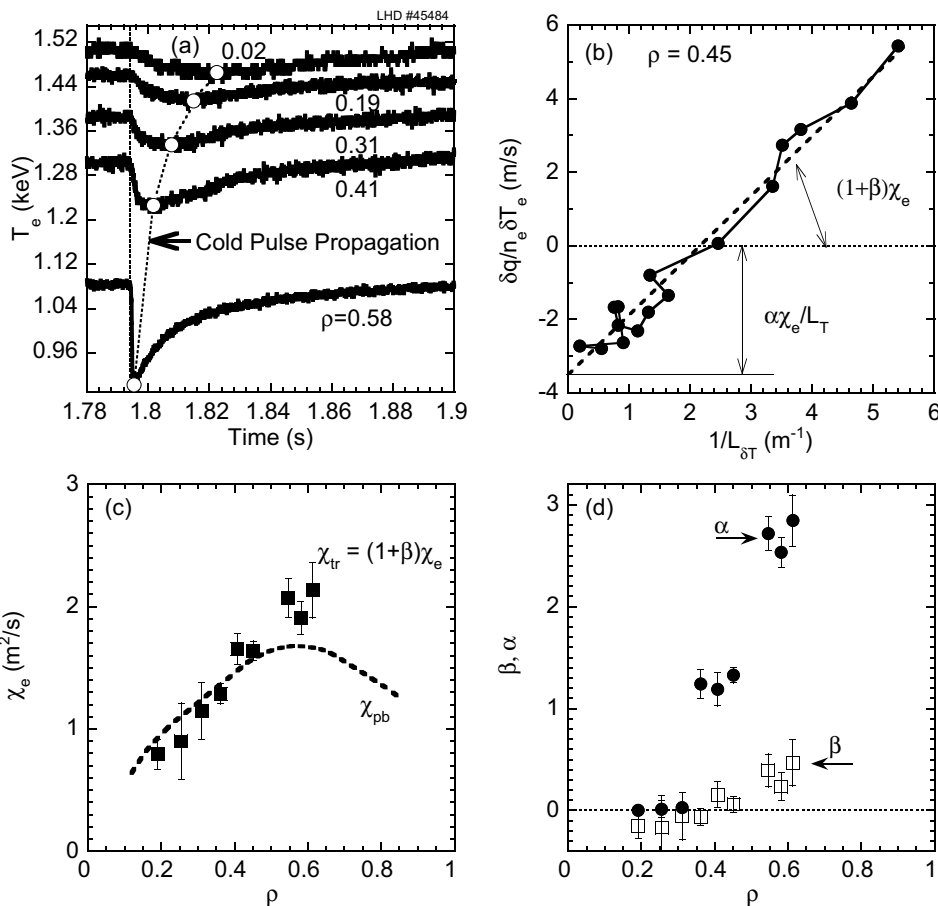


FIG. 2: (a) time evolution of T_e perturbations induced by TESPEL injection at different radii, (b) behavior of plasma at $\rho = 0.45$ in the perturbed gradient vs the perturbed heat flux space, (c) radial profiles of χ_{tr} and χ_{pb} , (d) radial profiles of β (the index of ∇T_e dependence of χ_e) and α (the index of T_e dependence of χ_e)

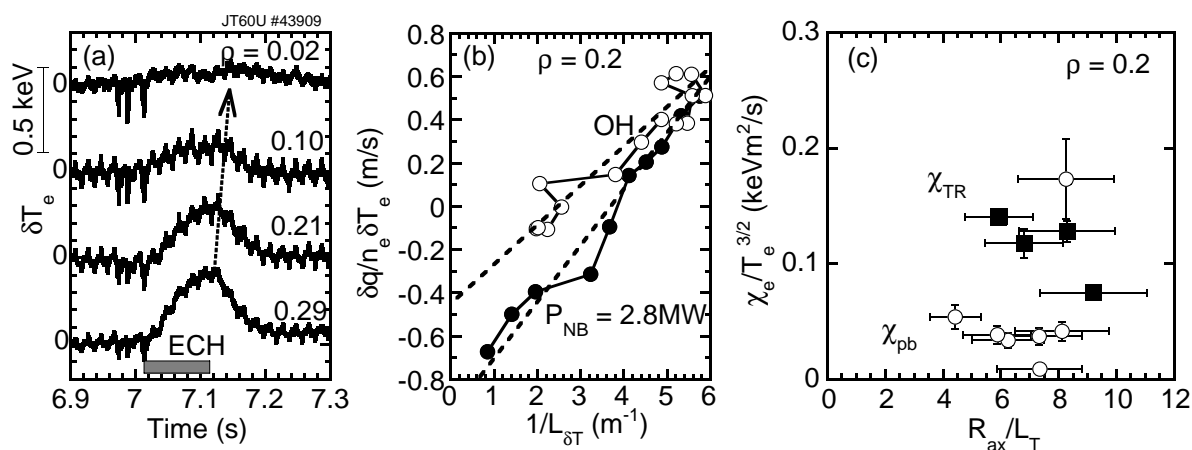


FIG. 3: (a) Time evolution of T_e perturbations induced by a step of the ECH in JT-60U ($\rho < 0.3$), (b) typical behavior of ohmic and NBI plasmas in the perturbed gradient and the perturbed heat flux space ($I_p = 0.8MA$), (c) R_{ax}/L_T dependence of χ_{pb} and χ_{tr} , here the χ_{pb} and the χ_{tr} are obtained in the density region of $n_{e0} = 1.6 - 2.5 \times 10^{19} m^{-3}$

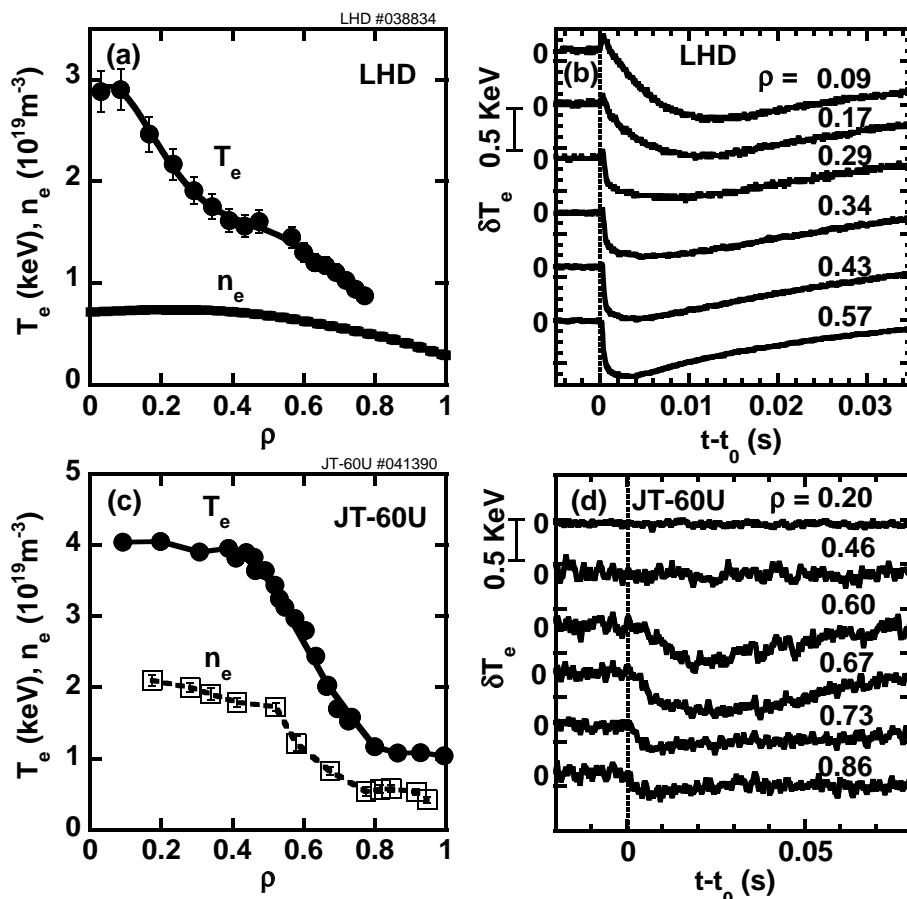


FIG. 4: Radial profiles of e-ITB plasmas just before TESPEL/Pellet injection in (a) LHD and (c) JT-60U, and time response of T_e to edge cooling in (b) LHD and (d) JT-60U. The TESPEL/Pellet is injected at $t = t_0$.

The transport barriers are considered to be formed by the suppression of turbulence-induced transport both in helical systems and tokamaks, however some important questions, such as whether the transport in the ITB is diffusive or convective and whether it is still stiff or not, have not been answered yet. Transient experiments are relevant for these issues to be clarified.

The e-ITB is formed when the ECH is focused on the magnetic axis in LHD ($P_{EC} \sim 0.8 \text{MW}$, $P_{NB} \sim 2 \text{MW}$, $R_{ax} = 3.5 \text{m}$, $a_p = 0.58 \text{m}$, $\bar{n}_e = 0.7 \times 10^{19} \text{m}^{-3}$), and it is formed in the reversed shear plasma [11] on JT-60U ($P_{NB} = 7.6 \text{MW}$, $R_{ax} = 3.4 \text{m}$, $a_p = 0.94 \text{m}$, $\bar{n}_e = 1.5 \times 10^{19} \text{m}^{-3}$, $I_p = 1 \text{MA}$). Typical time evolutions of cold pulse propagation and radial profiles of target plasmas are shown in Fig. 4. There is also an ion barrier ($T_{i0} = 7 \text{keV}$) in the JT-60U plasma, while neither ion nor n_e ITBs are present in LHD ($T_{i0} = 1.8 \text{keV}$). The cold pulse propagation technique is also used to perturb the ITB plasmas. The TESPEL (in LHD) and the pellet (in JT-60U) are injected to the edge of e-ITB plasmas. A unique feature of cold pulse propagation is observed. When the cold pulse approaches the ITB foot, the negative peak of the cold pulse is enhanced both in JT-60U and LHD as shown in Fig. 5 (a) and (b). Here, no evidence of a significant plasma shift induced by the TESPEL/PELLET injection is observed. In the JT-60U plasma, the cold pulse is damped strongly to zero further inside the ITB region, and thus there is no perturbation in the core. The cold pulse reaches to the core in LHD plasma, however, the slowing down of the cold pulse propagation inside the ITB is observed as shown in Fig. 4(b). In addition, the temperature

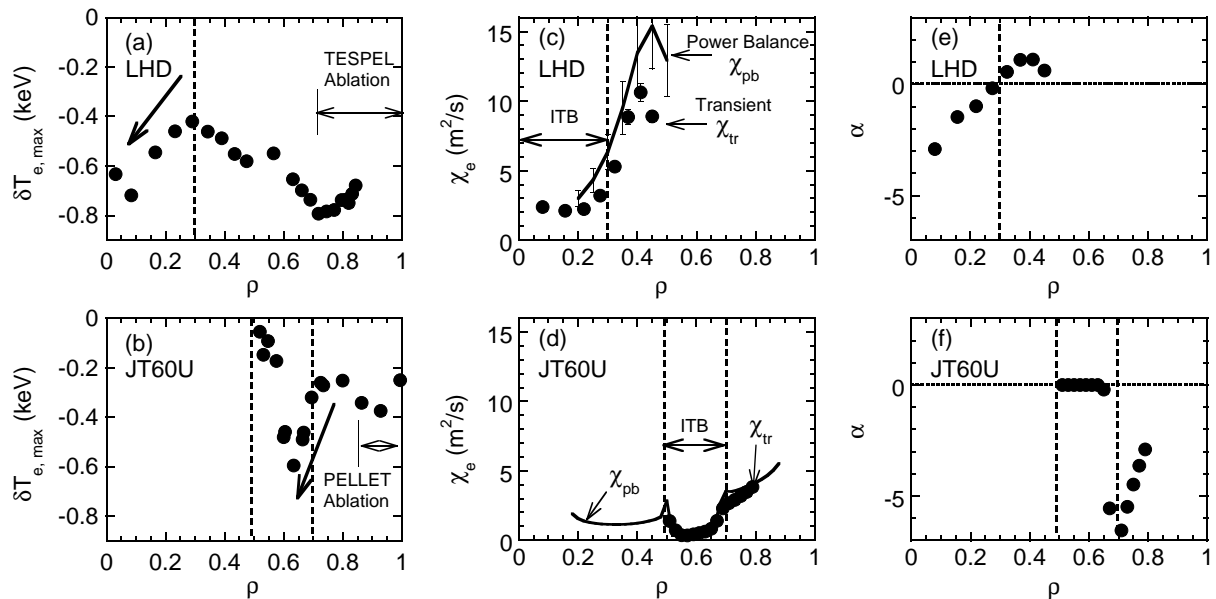


FIG. 5: Radial profiles of the cold pulse peak in (a) LHD and (b) JT-60U, the transient and powerbalance heat diffusivity in (c) LHD and (d) JT-60U and the T_e dependence factor of χ_e in (c) LHD and (d) JT-60U.

returns to the previous profile in spite of the increase in density after TESPEL/PELLET injection. Thus these enhancements of the cold pulse cannot be due to the backforward transition of the ITB. The simple diffusive nature (heat flux is proportional to temperature gradient) cannot explain this enhancement of the cold pulse. The non-linear dependence of χ_e on T_e and/or ∇T_e is required. Transient transport analysis shows the strong reduction of $\chi_{tr} = (1 + \beta)\chi_e$ inside the ITB region (see Fig. 5 (c) and (d)). The small difference between χ_{tr} and χ_{pb} indicates $\beta = 0$ (i.e. the ITB is in a “weak or not stiff” region). The vanishing of ∇T_e dependence of χ_e in JT-60U may be due to the strong reduction of the turbulence-driven-transport inside the ITB. The growth of the cold pulse peak can be explained by the convective-like term driven by the T_e dependence of χ_e (see Eq. 1) because the transient transport analysis indicates the strong negative T_e dependence of χ_e (χ_e decreases with an increase in T_e). Figure 5 (e) and (f) show the T_e dependence factor α of χ_e . The negative T_e dependence ($\alpha < 0$) is observed inside the ITB in LHD, while it is observed not only inside the ITB but also outside the ITB in JT-60U. The transport just outside the ITB region in JT-60U, where the flat T_e and q profiles are observed, may be different qualitatively from the transport shown in Fig. 3. Although the physical mechanisms that could be responsible for this negative T_e dependence of χ_e are unclear yet (any gyro-Bohm models can not provide $\alpha < 0$), the negative T_e dependence indicates the qualitative change in turbulence effects on transport. The q profile effect may be a key issue that should be clarified because both plasmas in Fig. 5 have the negative magnetic shear configuration.

4. Non-local effects in transport

Several recent experiments in LHD and JT-60U, however, point to the importance of non-local effects in the turbulent-induced transport [12]. Rapid cold pulse propagations are observed both in LHD and JT-60U. The typical time evolution of core temperature response to the edge cooling in JT-60U high- β_p ELMy H-mode plasma ($P_{NB} = 18\text{MW}$, $R_{ax} = 3.3\text{m}$, $a_p = 0.93\text{m}$, $\bar{n}_e = 3 \times 10^{19}\text{m}^{-3}$, $I_p = 1.8\text{MA}$) is shown in Fig. 6(a). The core T_e begin to decrease before

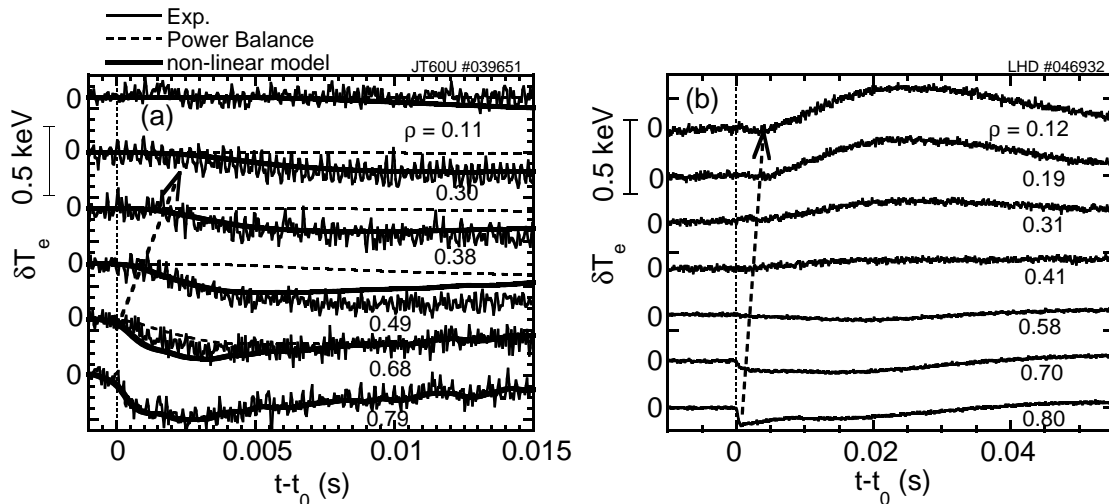


FIG. 6: Time evolution of T_e perturbations at different radii in (a) JT-60U high- β_p ELMy H-mode plasma and (b) LHD ECH + NBI plasma. The simulation results with the linear χ_e model ($\chi_e = \chi_e$ i.e. $\alpha = 0, \beta = 0$ in the non-linear model) and the non-linear χ_e model ($\alpha = 0, \beta = 9$) are also shown in (a). The TESPEL is injected at $t = t_0$.

diffusive transport effect (calculated by χ_{pb}) reaches this region, and the magnitude of cold pulse is larger than that predicted by diffusion. To explain this prompt response of core T_e by the non-linearity of χ_e , the strong ∇T_e dependence of χ_e is required (see simulation result in Fig. 6(a)). This strong ∇T_e dependence is not consistent with the power degradation observed in JT-60U. One of the non-linear but local models (e.g. ITG-based models [13]) can explain such a strong ∇T_e dependence, however, there is no evidence of rapid changes in the fluctuations or T_i profile.

It has been observed that the non-local response to edge cold pulses often have reversed polarity, with the core T_e increasing in response to edge cooling in many tokamaks [14, 15]. While such a phenomenon, which can not be explained by the local diffusive model even if the heat flux is a non-linear function of ∇T_e and T_e , has not been reported so far in helical systems. However, a first observation of the reverse of δT_e polarity in helical systems is done in LHD, and thus the strong non-local effects in helical systems is evident as well as in tokamaks. The typical T_e response to the edge cooling in LHD is shown in Fig. 6(b). The TESPEL is injected to the edge of plasma ($P_{EC} \sim 0.8\text{MW}$, $P_{NB} \sim 2\text{MW}$, $T_{e0} = 3\text{keV}$, $\bar{n}_e = 1 \times 10^{19}\text{m}^{-3}$, same magnetic configuration as Fig. 2). The cold pulse produced in the edge region ($\rho > 0.8$) is strongly reduced in the region of $0.4 < \rho < 0.6$, and thus neither T_e nor ∇T_e are changed significantly by the cold pulse propagation. In spite of no change in temperature and its gradient, a sudden rise of T_e is observed in the central region ($\rho < 0.4$). This indicates an abrupt reduction of χ_e unrelated to ∇T_e and/or T_e . Unfortunately, plasma goes back to normal condition after 20ms from TESPEL injection as well as in tokamaks. There are some discoveries in the characteristics of the non-local T_e rise observed in LHD, (1) The non-local T_e rise is also observed in plasmas sustained by pure ECH, (2) The formation of e-ITB is triggered by a non-local T_e rise in LHD when the plasma is heated by just below the critical power, (3) The non-local T_e rise is also observed in the e-ITB plasma. These new observations will help to make a physical picture of the turbulence, which can explain both non-linearity and non-locality in transport. Especially, observation (1) indicates the plasma current itself is irrelevant to the non-local transport mechanism. Moreover,

the similarities of the non-local T_e rise between tokamaks and LHD allow us to conclude that the magnetic shear is not important in the non-local transport. The non-local T_e rise in LHD is unclear in the high- n_e and low- T_e region ($n_e > 1.5 \times 10^{19} \text{m}^{-3}$, $T_e < 2.0 \text{keV}$) just as TFTR scaling predicts [15]. The non-local T_e rise, however, has not been observed in JT-60U even if n_e and T_e are in condition, which is predicted by TFTR scaling.

5. Summary

Cold/Heat pulse propagation experiments in LHD and JT-60U show the following electron heat transport features. (i) Cold pulses in no-ITB plasma in LHD ($\nu_* = 0.1 - 0.3$, $\rho_* = 3 - 4 \times 10^{-3}$) show a gyro-Bohm like T_e dependence of χ_e . On the other hand, heat pulse propagations show not only the gyro-Bohm like T_e dependence of χ_e but also the ∇T_e dependence of χ_e in the core region ($\rho < 0.3$) of JT-60U plasma ($\nu_* = 0.01 - 0.1$, $\rho_* = 4 - 10 \times 10^{-3}$). (ii) No or weak ∇T_e dependence inside the ITB is found both in LHD and JT-60U reverse shear plasmas. The negative T_e dependence of χ_e is found inside the ITB in LHD and inside and outside the ITB in JT-60U. (iii) The prompt cold pulse propagation in a high- β_p ELMy H-mode plasma in JT-60U and the reverse of cold pulse polarity in low density plasmas ($n_e < 1 - 1.5 \times 10^{19} \text{m}^{-3}$) are evidence for non-local heat transport.

Acknowledgments

The part of this work was carried out as a joint work under the Facility Utilization Program of JAERI.

References

- [1] F. Wagner *et al*, Phys. Rev. Lett. **56** (1986) 2187
- [2] J. D. Callen *et al*, Phys. Fluids B **4** (1992) 2142
- [3] H. Yamada *et al*, Nucl. Fusion **43** (2003) 749
- [4] W. Horton *et al*, Phys. Fluids **31** (1988) 2971
- [5] F. Romanelli and S. Briguglio, Phys. Fluids **B 2** (1990) 754
- [6] F. Ryter *et al*, Phys. Rev. Lett. **86** (2001) 5498
- [7] N. J. Lopes Cardozo, Plasma Phys. Control. Fusion **37** (1995) 799
- [8] S. Sudo *et al*, Plasma Phys. Control. Fusion **44** (2002) 129
- [9] K. Tanaka, this conference
- [10] R. Waltz and A. Boozer, Phys. Fluids B **5** (1993) 2201
- [11] T. Fujita, Phys. Rev. Lett. **78** (1997) 2377
- [12] S. V. Neudatchin, Plasma Phys. Control. Fusion **44** (2002) A383
- [13] M. Kotschenreuther *et al*, Phys. Plasmas **2** (1995) 2381
- [14] K. W. Gentle *et al*, Phys. Rev. Lett. **74** (1995) 3620
- [15] M. W. Kissik *et al*, Nucl. Fusion **38** (1998) 821